Available online at www.sciencedirect.com
ScienceDirect
Journal of Power Sources 174 (2007) 1137–1141
JOURNAL OF POWER SOURCES
www.elsevier.com/locate/jpowsour

Short communication

Chemically oxidized manganese dioxides for lithium secondary batteries

Won Il Jung *, Kazuyuki Sakamoto, Cédric Pitteloud, Noriyuki Sonoyama, Atsuo Yamada, Ryoji Kanno

Department of Electronic Chemistry, Interdisciplinary Graduate School of Science and Engineering, Tokyo Institute of Technology, 4259 Nagatsuta, Midori-ku, Yokohama 226-8507, Japan

Available online 26 June 2007

Abstract

The specific discharge capacity of γ-MnO_2 was improved with chemical oxidation and vacuum-drying processes. The intergrowth structure and electrochemical performance were studied by X-ray diffraction and electrochemical measurements; the structure–electrochemical property relationships were clarified. Vacuum-dried γ-MnO_2 showed structural changes with capacity fade as the temperature increased, while the chemically oxidized γ-MnO_2 showed no structural change without any capacity fading. The latter material showed a first discharge capacity of 275 mAh g^{-1}, and a reversible capacity of 250 mAh g^{-1} with two discharge plateaux after second cycle, which is the highest capacity among the γ-MnO_2 prepared previously.

Keywords: Manganese dioxide; Chemical oxidation; Lithium secondary battery

1. Introduction

Manganese dioxides are of interest as the positive electrode material not only for primary batteries but also for secondary lithium batteries due to their high capacity and low toxicity, especially, γ-MnO_2 has good electrochemical performances [1–5]. The structures of γ-MnO_2 are built up of chains of edge-sharing MnO_6 octahedra that share corners to form channels through the structure and have an intergrowth of pyrolusite (1 × 1 channels) and ramsdellite (2 × 1 channels) structures. These channels can store Li ions in the structure and make it easy to be inserted and extracted during the charging and discharging [4].

γ-MnO_2 has the structural defects described by the pyrolusite–ramsdellite intergrowth and the microtwinning defect. The random intergrowth of pyrolusite and ramsdellite structure in γ-MnO_2 was studied by De Wolff, and the amount of pyrolusite intergrowth was denoted as P_r [6]. Chabre and Pannetier introduced the parameter M_t, which represents the microtwinning generated by twinning planes in both pyrolusite and ramsdellite domains [7,8].

Another structural characteristic of γ-MnO_2 is the existence of cation vacancies and protons in the structure [9,10]. Ruetschi proposed that there are vacancies in the Mn^{4+} sublattice in the MnO_2 and each empty Mn^{4+} site is coordinated to four protons in the form of OH^- ions to compensate the charge of the manganese ions. These types of protons are called "Ruetschi" protons that are thought to be localized in the vacancy octahedron and be permanently occupied [11,12]. Protons located in conjunction with Mn^{3+} ions in the structure are called "Coleman" protons [13]. Therefore, the chemical composition of γ-MnO_2 could be explained by this formulation: $Mn_{1-x-y}{}^{4+}Mn_y{}^{3+}\square_x O_{2-4x-y}{}^{2-}(OH)_{4x+y}{}^-$, where □ denotes cation vacancy [7].

Heat-treatment causes dehydration in the inorganic structure. However, in the case of γ-MnO_2 there occurs structural change during heat-treatment above 150 °C, which is described by the increase of P_r and decrease of M_t [14]. Moreover, this structural change induces poor cyclability on cell performances.

Chemical oxidation is known to be useful to remove cations in the structure and $NO_2{}^+$ is potentially effective oxidizing agent in acetonitrile solution [15–18]. They can oxidize not only protons in conjunction with Mn^{3+} ions but also protons near Mn vacancies in the structure. It can be thought to enlarge the specific capacity of the material.

In this study, chemical oxidation treatment with vacuum-drying process was performed to improve the specific charge–discharge capacity of commercially available γ-MnO_2. To compare the effect of chemical oxidation with vacuum-drying

* Corresponding author.
E-mail address: wjung@echem.titech.ac.jp (W.I. Jung).

0378-7753/$ – see front matter © 2007 Elsevier B.V. All rights reserved.
doi:10.1016/j.jpowsour.2007.06.098

process, we analysed the structure change after the both treatments on γ-MnO_2 samples. Electrochemical properties of chemically oxidized γ-MnO_2 were investigated to make the correlation between structural change and cell performance.

2. Experimental

Electrolytic manganese dioxides were used as raw materials (Mitsui Kinzoku, product name TKV-B). These were heat-treated in vacuum condition at temperatures ranging from 150 to 500 °C for 12 h, and were kept under argon gas atmosphere for several days.

For the chemically oxidized samples, electrolytic manganese dioxides were firstly heated at 100 °C for 12 h in vacuum condition in order to remove water. After heat-treatment, samples were mixed with an oxidant (NO_2BF_4) in molar ratio of γ-MnO_2/NO_2BF_4 = 1/1 in acetonitrile solution and stirred for 24 h under argon gas atmosphere. Followed by filtering and vacuum-drying process at 120 °C for 12 h, these were kept under argon gas atmosphere for several days.

The electrochemical characterizations were performed using 2032 coin-type cell. The cathode materials were mixed with acetylene black and Teflon powder with the gravimetric ratio of about 50:10:2.5, and pelletized with a size of 1 cm^2. Cells were composed by stacking cathode pellet between two Al mesh and Li foil as an anode separated by polypropylene separator soaked in electrolyte (1 M $LiPF_6$ with EC/DEC = 3:7 vol.%). Cells were assembled in an argon atmospheric glove box. The

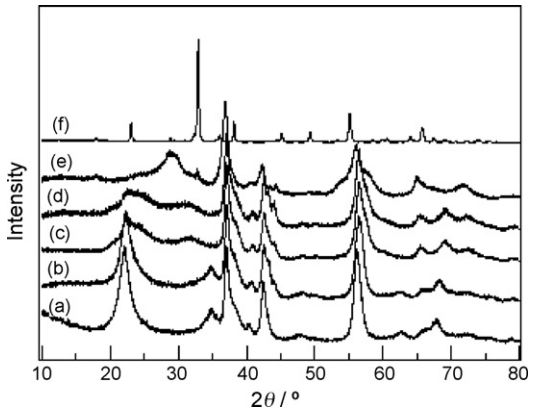

Fig. 1. X-ray powder diffraction patterns for γ-MnO_2 materials obtained by vacuum-drying treatment: (a) no-treated, (b) 150 °C, (c) 200 °C, (d) 300 °C, (e) 400 °C, and (f) 500 °C.

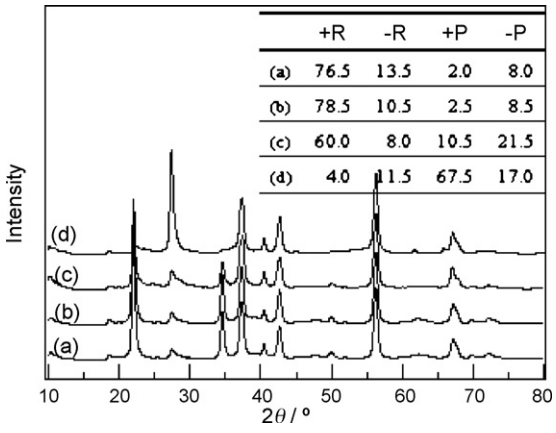

Fig. 2. X-ray diffraction patterns calculated by DIFFaX simulation, and their structural transformation parameters for γ-MnO_2 with various vacuum-drying temperatures: (a) raw material, (b) 200 °C, (c) 300 °C, and (d) 400 °C.

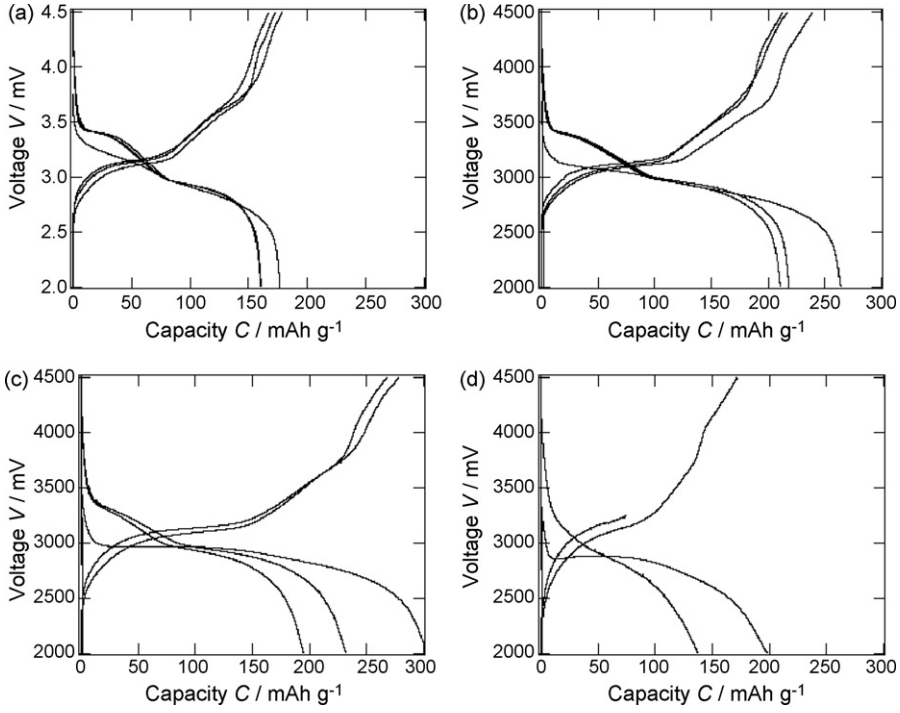

Fig. 3. Charge–discharge profiles of γ-MnO_2 materials obtained by vacuum-drying process at various temperatures: (a) 100 °C, (b) 150 °C, (c) 300 °C, and (d) 400 °C.

charge–discharge experiments were examined over a voltage range of 2.0–4.5 V versus Li/Li^+ with a current density of 0.1 mA cm^{-2} at 25 °C.

Powder X-ray diffraction analysis (XRD, Rigaku RU200B) was used for the structure characterization of γ-MnO_2. Patterns were recorded over the 2θ range 10–80° with a step size of 0.03° and a count time of 3.0 s. We estimated P_r value with the method proposed by Chabre and Pannetier [7]. Structural transformation parameters were also investigated using a program DIFFaX with a model containing stacking fault in the layered structure [14,19].

3. Results and discussion

The X-ray powder diffraction diagrams of γ-MnO_2 treated by vacuum drying are shown in Fig. 1. The diffraction patterns changed as the heat-treatment temperature increased from ambient temperature to 400 °C. The diffraction peaks of (1 1 0) ($2\theta \cong 22°$) and (1 3 0) ($2\theta \cong 36°$) disappeared and a new peak appeared around $2\theta \cong 29°$. The (1 3 1) peak ($2\theta \cong 48°$) disappeared. Moreover, the peak around $2\theta \cong 56°$ was clearly separated into two, and each peaks were indexed as (0 2 1) and (1 2 1). These changes correspond to a transformation from the ramsdellite to the pyrolusite structure. At 500 °C, the diffraction pattern changed due to a conversion from γ-MnO_2 to Mn_2O_3.

There are two types of stacking directions in the ramsdellite structure, +R and −R, and the ratio of +R/−R is relative quantities of left and right structure twinned on the (0 2 1) plane. There are parameters, +P and −P, in the pyrolusite similar to +R and −R in the ramsdellite structure [7]. Structural transformation of γ-MnO_2 can be expressed by a combination of four kinds of layer vectors +R, −R, +P and −P. Fig. 2 shows the simulated diffraction patterns together with the parameters used for the calculation. With increasing temperature up to 300 °C, the ratio of +R decreased and +P and −P increased. At 400 °C, the ratio of +P suddenly increased and −P decreased. The heat-treatment process caused the main stacking vector change from +R to −P, and finally to +P [14]. Although these structural considerations have limitations to confirm the changes in stacking sequence and twin (0 2 1) plane along one-dimensional direction, the structure changes with the heat-treatment process are well described for the γ-MnO_2.

Fig. 3 shows the charge–discharge profiles of γ-MnO_2 as a function of vacuum-drying temperature. The first discharge capacity increased as vacuum-drying temperature increased up to 300 °C, and the average voltage of the first discharging profile and cycle performance decreased. With increasing temperature up to 400 °C, discharging capacity, average voltage, first discharging potential and cycle performance suddenly decreased. These changes of cell performances could be related to the structural changes of γ-MnO_2. The first discharging curve of the sample heat-treated at 100 °C (Fig. 3(a)) has two plateaux around 3.3 and 3.0 V, which corresponds to the sites around the Mn^{4+} vacancy and the "Ruetschi" protons, and the sites associated with Mn^{3+} in the tunnels of pyrolusite and ramsdellite structure, respectively [12,20,21]. As the temperature increased over 150 °C (Fig. 3(b)–(d)), the plateau around 3.3 V of the first discharging curve disappeared. The heat-treatment of γ-MnO_2 caused the structural change from ramsdellite to pyrolusite, and collapsed the Li-inserting sites around the Mn^{4+} vacancy and the "Ruetschi" protons. This is consistent with the results of X-ray diffraction analysis.

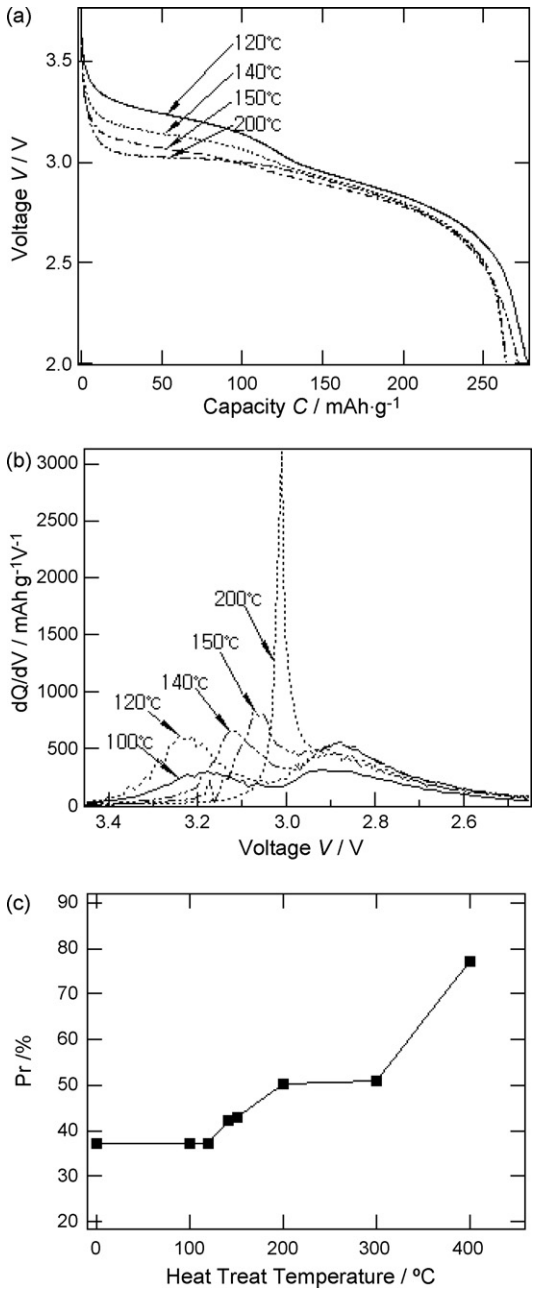

Fig. 4. (a) First discharge profiles, (b) differential capacity curves of first discharge and (c) P_r values at various temperatures of chemically oxidized γ-MnO_2 with various vacuum-drying temperatures.

The relationship between the cell performance and vacuum-drying condition of chemically oxidized γ-MnO_2 will be discussed. Fig. 4 shows the first discharge profiles, their differential capacity curves, and structural values of P_r of chemically oxidized γ-MnO_2 at various vacuum-drying temperatures. Two plateaux were clearly observed for the first discharging profile of the sample treated at 120 °C, which is similar to the conventional discharging profile of γ-MnO_2. However, with increasing tem-

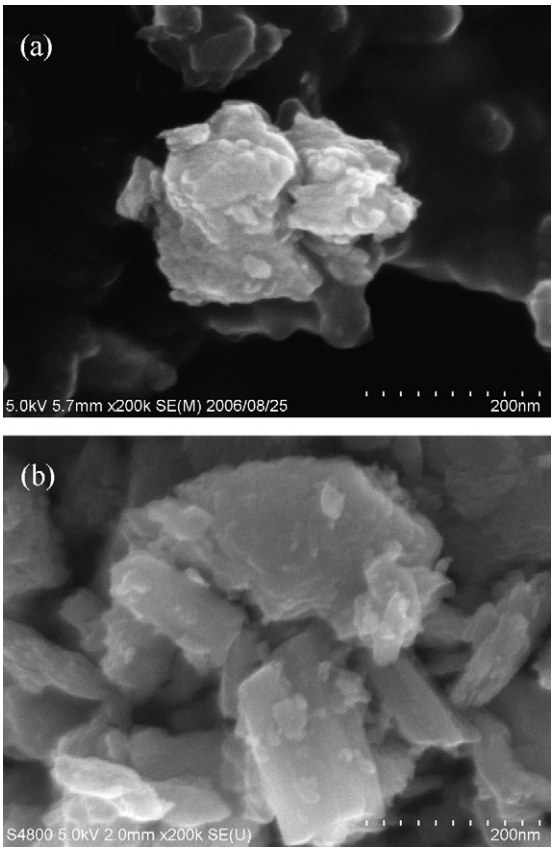

Fig. 5. SEM images of γ-MnO_2: (a) no-treated γ-MnO_2 and (b) chemically oxidized γ-MnO_2.

perature, the potential of the plateau around 3.3 V decreased, and finally disappeared at 200 °C. The changes of the plateau around 3.3 V are clearly observed for the differential capacity curves (dQ/dV) shown in Fig. 4(b). Two peaks were clearly observed for the sample of 120 °C, and the peak around 3.2 V shifted to lower voltage, and finally, two peaks around 3.2 and 2.85 V became one peak around 3.0 V at 200 °C. These changes are consistent with the increase in the parameter P_r in Fig. 4(c). The structural change from ramsdellite to pyrolusite affects the Li site.

Fig. 5 shows SEM photographs of γ-MnO_2 before and after the chemical oxidation process. These samples were composed of secondary particles of about 200–300 nm agglomerated with primary particles of about 20 nm. There was no apparent difference between the two samples, indicating that the chemical oxidation process did not affect the shape of γ-MnO_2 particles.

Fig. 6 shows volumetric adsorption isotherms of N_2 and BET surface areas on γ-MnO_2. The surface areas of γ-MnO_2 before and after the chemical oxidation process were 51.9 and 45.9 $m^2\,g^{-1}$, respectively. The N_2 adsorption curves of the two γ-MnO_2 increased when the relative pressure was increased up to 0.5, and no significant difference in the adsorption isotherm profiles was observed between two materials at all pressure ranges. The surface areas of the two materials are almost the same. Moreover, these results of SEM and BET measurements demonstrated no changes in the morphology in γ-MnO_2 during chemical oxidation process.

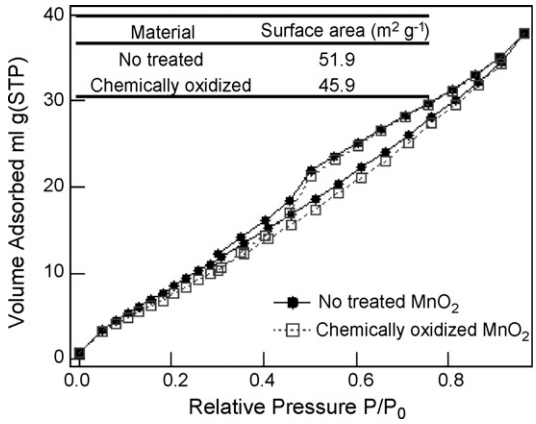

Fig. 6. N_2 adsorption–desorption isotherms and BET surface areas for no-treated γ-MnO_2 and chemically oxidized γ-MnO_2.

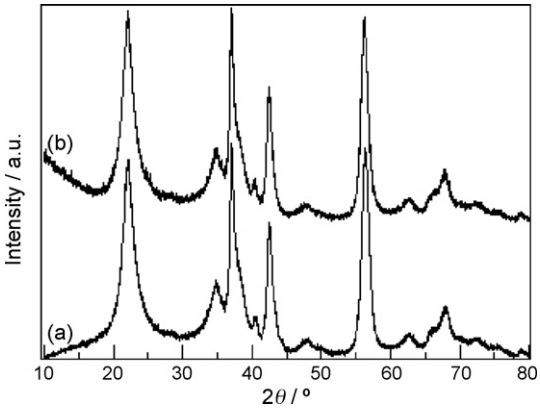

Fig. 7. X-ray powder diffraction diagrams for γ-MnO_2: (a) no-treated γ-MnO_2 and (b) chemically oxidized γ-MnO_2.

Fig. 7 shows the X-ray powder diffraction diagrams for no-treated γ-MnO_2 and chemically oxidized γ-MnO_2 with vacuum-drying process at 120 °C. These patterns are similar to those of conventional EMD [7]. No significant structural changes were observed during chemical oxidation process, and protons were removed without any changes in the structure of γ-MnO_2 by the chemical oxidation process.

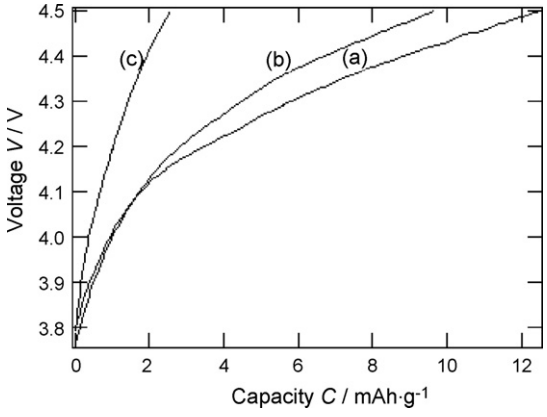

Fig. 8. First charge profiles of γ-MnO_2: (a) no-treated γ-MnO_2, (b) vacuum-dried γ-MnO_2 at 120 °C, and (c) chemically oxidized γ-MnO_2.

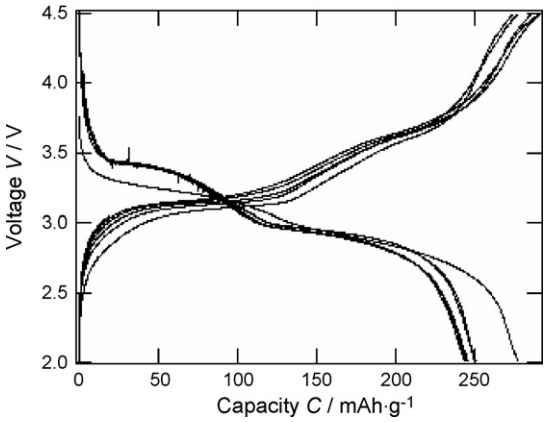

Fig. 9. Charge–discharge profiles of chemically oxidized γ-MnO_2 at optimized condition.

Fig. 8 shows the first charging profiles of no-treated γ-MnO_2, vacuum-dried γ-MnO_2, and chemically oxidized γ-MnO_2 with the upper cut-off voltage of 4.5 V. The charging profiles of γ-MnO_2 showed the deintercalation of remaining protons in the structure. Charge capacity of γ-MnO_2 decreased by vacuum-drying process, which indicates that a part of "Coleman" protons was removed by the heat-treatment [13,14]. The chemically oxidized γ-MnO_2 showed the first charging capacity of 3 mAh g^{-1}, which indicates that most of the protons concerned with electrochemical (de)intercalation were removed from the structure by chemical oxidation process.

Fig. 9 shows the charge–discharge profiles of chemically oxidized γ-MnO_2 treated by the optimized condition as follows: chemical oxidation for 24 h at 25 °C followed by filtering under argon atmosphere and vacuum-drying process at 120 °C. The cell showed a first discharge capacity of about 275 mAh g^{-1}, and a reversible capacity of about 250 mAh g^{-1} with two discharge plateaux after second cycle. The discharging capacity at the sixth cycle showed about 244 mAh g^{-1}, which is the highest capacity among the γ-MnO_2 prepared previously.

4. Conclusions

Specific discharging capacity of γ-MnO_2 was improved by chemical oxidation treatment and vacuum-drying process. These treatments provided the highest capacity of about 275 mAh g^{-1} for the first discharge and a reversible capacity of 250 mAh g^{-1} after the second discharge. The structure changed from ramsdellite to pyrolusite with increasing vacuum-drying temperature. The structural transformation was studied by DIFFaX simulation, which shows the stacking vector change from +R to −P, and finally to +P with the heat-treatment. The increase in the capacity for the chemically oxidized γ-MnO_2 corresponds to the removal of "Ruetschi" protons by the strong oxidation process. The γ-MnO_2 showed high reversible charge–discharge capacity, and is a promising candidate for positive materials for lithium batteries.

References

[1] A. Sasaki, A. Kozawa, J. Electrochem. Soc. Jpn. 25 (1957) 115.
[2] A.F. Wells, Structural Inorganic Chemistry, Fifth ed., Oxford University Press, 1984.
[3] G. Pistoia, A. Antonini, J. Electochem. Soc. 144 (1997) 1553.
[4] P.M. De Wolff, Acta Crystallogr. 12 (1959) 341.
[5] S. Sarciaux, A. Le Gal La Salle, A. Verbaere, Y. Piffard, D. Guyomard, J. Power Sources 81/82 (1999) 656.
[6] J. Pannetier, Batteries Battery Mater. 11 (1992) 51.
[7] Y. Chabre, J. Pannetier, Prog. Solid State Chem. 23 (1995) 1.
[8] S. Sarciaux, A. Le Gal La Salle, A. Verbaere, Y. Piffard, D. Guyomard, J. Mater. Res. Soc. Symp. Proc. 548 (1999) 251.
[9] J. Fitzpatrick, L.A.H. Maclean, D.A.J. Swinkels, F.L. Tye, J. Appl. Electrochem. 27 (1997) 243.
[10] F. Fillaux, C.H. Cachet, H. Ouboumour, J. Tomkinson, C. Levy-Clement, L.T. Yu, J. Electrochem. Soc. 140 (1993) 585.
[11] P. Ruetschi, J. Electrochem. Soc. 131 (1984) 2737.
[12] P. Ruetschi, J. Electrochem. Soc. 135 (1988) 2657.
[13] P. Ruetschi, R. Giovanoli, J. Electrochem. Soc. 135 (1988) 2663.
[14] M. Nagao, C. Pitteloud, T. Kamiyama, T. Otomo, K. Itoh, T. Fukunaga, R. Kanno, J. Electrochem. Soc. 152 (2005) E230.
[15] K. Vidyasagar, J. Gopalakrishnan, J. Solid State Chem. 42 (1982) 217.
[16] N. Kumada, S. Muramatu, F. Muto, N. Kinomura, S. Kikkawa, M. Koizumi, J. Solid State Chem. 73 (1988) 33.
[17] A. Mendiboure, C. Delmas, P. Hagenmuller, Mater. Res. Bull. 19 (1984) 1383.
[18] G.M. Anderson, J. Iqbal, D.W.A. Sharp, J.M. Winfield, J.H. Cameron, A.G. McLeod, J. Fluorine Chem. 24 (1984) 303.
[19] M.M.J. Treacy, J.M. Newsam, M.W. Deem, Computer Code DIFFaX, Version 1.807.
[20] M.M. Thackeray, Prog. Solid St. Chem. 25 (1997) 1.
[21] D. Balachandran, D. Morgan, G. Ceder, A. van de Walle, J. Solid State Chem. 173 (2003) 462.